

# WATER PUMPING SYSTEM FROM PHOTOVOLTAIC CELLS USING A CURRENT-FED PARALLEL RESONANT PUSH-PULL INVERTER

Denizar Cruz Martins, Marcello Mezaroba and Ivo Barbi  
Federal University of Santa Catarina

Department of Electrical Engineering

Power Electronics Institute - INEP

P.O. BOX 5119 - 88040-970 - Florianópolis - SC - Brasil

Phone: 55(48) 231-9204 - Fax: 55(48) 234-5422

## ABSTRACT

This paper presents the analysis of a water pumping system from photovoltaic cells using a current-fed parallel resonant push-pull inverter, for residential applications in rural areas. The power structure is particularly simple and robust. It works with a ZVS commutation. Its main features are: one power processing stage, simple control strategy, lower harmonic distortion of the load voltage and natural isolation. The principle of operation, design procedure and experimental results are presented.

## I. INTRODUCTION

The increasing research of alternative means for obtaining electrical energy in a simple manner, without pollution, that at the same time do not cause a hard ecologic impact on the environment, has led some professionals of the Electrical Engineering area to opt for solar energy conversion.

This kind of energy, apparently unfailling, presents a series of advantages, among them we can point out: non aggression to natural conditions, and no cause of any type of pollution. However, its treatment for industrial applications and even for residential ones, represents yet a relatively high cost. Nowadays, the studies of the conception and materials manufacture area for photovoltaic cells are rapidly being developed with great success. The main objective is to obtain systems for converting solar energy into electrical energy in a simple, cheap, and safe way.

Many works for residential applications are available in technical literature [1,2,3]. Their power circuits are somewhat sophisticated and use many controlled switches.

Considering the objective mentioned above, this paper describes a system for residential applications in a rural areas, where power from a utility is not available or is too costly to install. The system consists of a water pumping from photovoltaic cells using a current-fed parallel resonant push-pull inverter with battery storage.

The power structure proposed in this paper is particularly simple and robust. It works in a ZVS commutation. Its main features are: one power processing stage, simple control strategy, lower harmonic distortion of the load voltage, natural isolation and low number of controlled switches.

## II. EQUIVALENTE ELECTRIC MODEL OF THE WATER PUMP

The pump used was an under-water vibratory pump. This kind of pump is very used due its simplicity, low cost, and robustness. Besides, this pump can effectuate the pumping in well with profundity around 80 meters. In normal conditions the pumping is approximately 1500 liters per hour. In Fig.1 we can observe the behavior of the pump for various profundities.

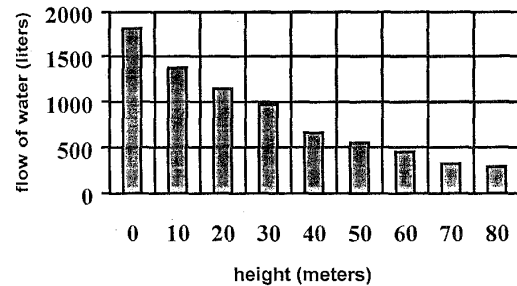


Fig. 1 - Performance of the pump

The technical characteristics of the pump are shown in Table 1.

Table 1: Technical characteristics of the pump.

Model	BK N° 3 - 80m
System	Vibratory
Apparent Power	1,100 VA
RMS Voltage	220 V
Frequency	60 Hz
Pressure Tube	3/4"
Weight	5.5 Kg
Flow of Water	1800 liters

The equivalent electric model is obtained experimentally, connecting the pump directly in the utility. Figs 2 and 3 show the waveforms of the voltage and current in the pump. The equivalent electric model is presented in Fig.4.

$$V_{in} = 217.8 \text{ V (Utility rms voltage)}$$

$$I_p = 4.9 \text{ A (Pump rms current)}$$

$$\phi = 74.68^\circ \text{ (Phase angle)}$$

$$f = 60 \text{ Hz (Operation frequency)}$$

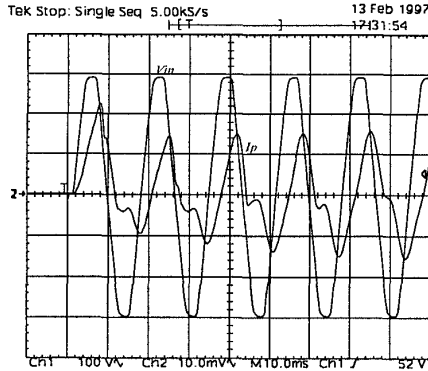


**Fig.2. – Voltage and current in the pump (Start condition)**  
Scale: 100V/div; 5A/div; 10ms/div

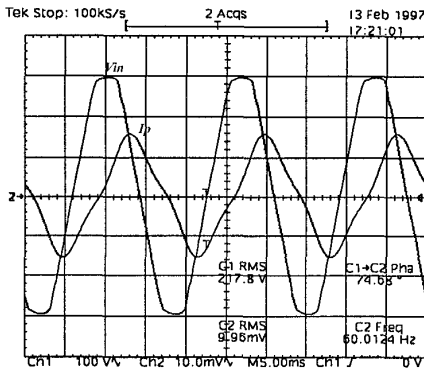


**Fig.3. – Voltage and current in the pump (Steady-state condition)**  
Scale: 100V/div; 5A/div; 5ms/div

We can verify that the load (pump) has a inductive characteristic, with a large circulation of reactive energy and low power factor ( $\cos\phi$ ). Therefore, the electric model can be easily represented by an equivalent parallel RL circuit (Fig.4), where:

$$R_p = \frac{V_{in}}{I_p \times \cos\phi} = 170\Omega \quad (1)$$

$$L_p = \frac{V_{in}}{2 \times \pi \times f \times I_p \times \sin\phi} = 120mH \quad (2)$$

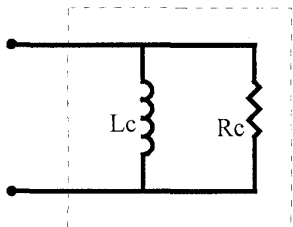


**Fig. 4 – Electric model of the pump.**

### III. PRINCIPE OF OPERATION

Considering the application mentioned in this paper, the Current-Fed Self-Oscillator Parallel Resonant Push-Pull Inverter is proposed [4,5], of which the resonant capacitor is connected in parallel with the load (pump), in the secondary side of the transformer. Mosfet's were used for the main switches, simplifying the self-oscillator drive circuit. The complete structure, including the self-oscillator drive circuit, is shown in Fig.5. To simplify the analysis, the following assumptions are made: the operation of the circuit is steady-state; the semiconductors are considered ideal; the transformer is represented by its magnetizing inductance; and the input current is maintained constant without ripple. The parallel resonant push-pull inverter has two operation stages shown in Figs. 6 and 7.

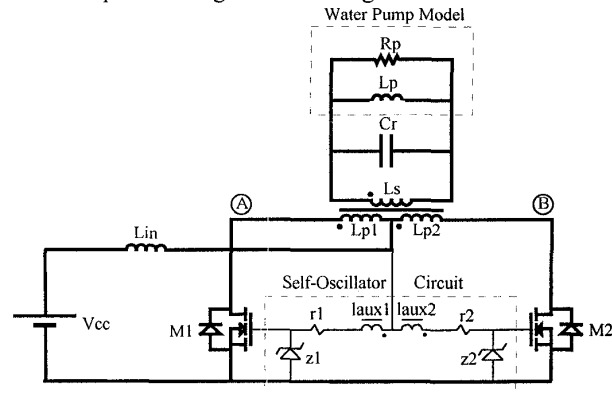


**Fig. 5 – Proposed Structure.**

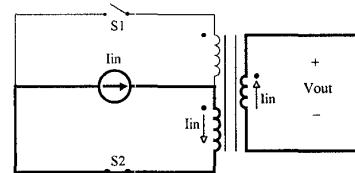


**Fig. 6 – 1<sup>st</sup> stage.**

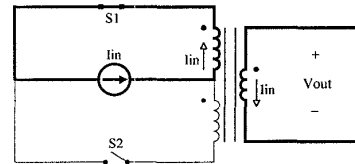


**Fig. 7 – 2<sup>nd</sup> stage.**

Operation Stages:

**1<sup>st</sup> Stage ( $t_0, t_1$ )** - Fig. 6: This stage start at  $t=t_0$ . When the voltage  $V_{out}$  reaches zero, the switch  $S_1$  turns off and the switch  $S_2$  turns on instantaneously. The commutation of the switches occur at the zero voltage.

Due to the resonance between  $C_r$  and  $L_p$ ,  $V_{out}$  increases sinusoidally.

2<sup>nd</sup> Stage ( $t_1, t_2$ ) - Fig. 7: By the time  $t_1$ , the switch  $S_2$  turns off and the switch  $S_1$  turns on. The voltage  $V_{out}$  decreases sinusoidally until the time  $t_2$ , where a new operation period begin.

The main waveforms are shown in Fig.8.

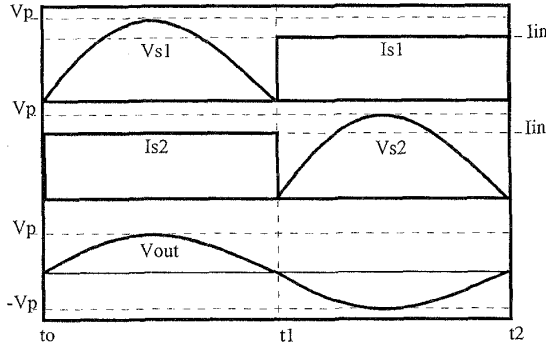


Fig.8. – Main Waveforms.

#### IV. DESIGN PROCEDURE AND EXAMPLE

##### IV.1. Specifications:

###### Input Data:

$V_{cc} = 12V$  (Converter input voltage)

###### Water Pump Data:

$V_{out} = 220$  (rms voltage)

$S_{out} = 1085$  VA (apparent power)

$P_{out} = 281$  W (active power)

$L_p = 120$  mH (equivalent parallel inductance)

$R_p = 170 \Omega$  (equivalent parallel resistance)

$f = 60$  Hz (operation frequency)  $\Rightarrow \omega d = 377$  rad/s

$\eta = 80\%$  (efficiency)

##### IV.2. RMS $V_{AB}$ voltage.

The rms  $V_{AB}$  voltage is given by the following equation [5].

$$V_{AB(rms)} = \frac{V_{cc} \times \pi}{\sqrt{2}} = 26.65 V \quad (3)$$

##### IV.3. Transformer Turns Ratio (a).

$$a = \frac{V_{out(rms)}}{V_{AB(rms)}} = 8.25 \quad (4)$$

##### IV.4. Magnetizing inductance referred to the secondary side of the transformer ( $L_{m_{sec}}$ )

$$I_{m_{sec}} = 0.1 \cdot \frac{S_{out}}{V_{out}} \quad (5)$$

$$L_{m_{sec}} = \frac{V_{AB(rms)}}{\omega d \cdot I_{m_{sec}}} = 4.85 H \quad (6)$$

where  $I_{m_{sec}}$  is the magnetizing current referred to the secondary side of the transformer.

##### IV.5. Input current and inductor ( $I_{in}, L_{in}$ ).

$$I_{in} = \frac{V_{AB(rms)} \cdot a^2 \cdot \pi}{R_p \cdot \sqrt{2} \cdot h} = 29.7A \quad (7)$$

$$L_{in} = \frac{V_{cc} \cdot T/4}{0.1 \cdot I_{in}} = 18 mH, \quad (8)$$

where:  $T = 1/f$

##### IV.6. Resonant Capacitor ( $C_r$ ).

$$C_r = \frac{4.R_p^2 + \sqrt{16.R_p^4 - 16.R_p^2 \cdot L_{eq}^2 \cdot \omega d^2}}{8.R_p^2 \cdot L_{eq} \cdot \omega d^2} = 58.7 \mu F \quad (9)$$

where:  $L_{eq} = L_p // L_{m_{sec}}$

##### IV.7. Number of Parallel Batteries .

The average power and current delivery by the batteries will be:

$$P_{Bav} = \frac{P_{out}}{\eta} \cong 350W \quad (10)$$

$$I_{Bav} = \frac{P_{Bav}}{V_{cc}} \cong 30A \quad (11)$$

The number of parallel batteries is given by:

$$N_B = \frac{B_A \cdot I_{Bav}}{B_c} = 1.5 \text{ batteries} \quad (12)$$

where:

$N_B \rightarrow$  minimum number of parallel batteries,

$B_A \rightarrow$  battery autonomy: 3 hours;

$B_c \rightarrow$  battery capacity: 60Ah (one hour rate).

Two lead-acid batteries (12V - 100Ah (20 hour rate)) were chosen.

##### IV.8. Number of Photovoltaic Modules.

The photovoltaic modules used in this project can deliver 3Ah (Ampere hours) with a solar radiation of 1.000 W/m<sup>2</sup>. In the worst case the average solar radiation, in our region (Florianópolis/Santa Catarina – Brazil), is about 2500 W/m<sup>2</sup> per day. Thus:

$$Ah_d = \frac{I_{RS} \cdot R_{av}}{R_s} = 7.5 \text{ Ah} \quad (13)$$

where:

$Ah_d \rightarrow$  Ampere-hours delivery per photovoltaic module for one a day.

$R_{av} \rightarrow$  average solar radiation: 2500 W/m<sup>2</sup> / day (worst situation),

$R_s \rightarrow$  standard solar radiation: 1000 W/m<sup>2</sup>,

$I_{RS} \rightarrow$  delivery of current by the photovoltaic module for the  $R_{av}$  radiation: 3Ah.

Thus, the number of photovoltaic modules is given by:

$$N_p = \frac{Ah_L}{Ah_d} = 4 \text{ photovoltaic modules} \quad (14)$$

where:

$Ah_L \rightarrow$  Ampere-hours delivery to the load per day.

## V. SIMULATION RESULTS

With the objective of evaluating the employed methodology, some numerical simulations of the system were made using the PSPICE program [6], following the same specifications and the same design outlined in the preceding section.

The main results are shown in the following figures.

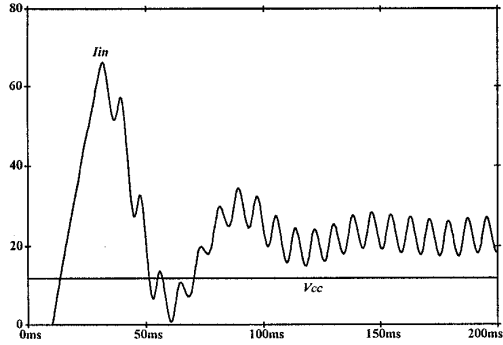


**Fig. 9 – Voltage and current in the batteries (Start-up transient).**

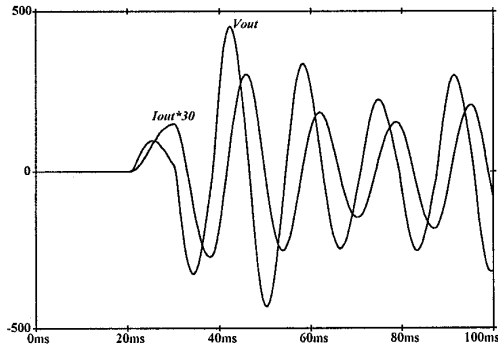


**Fig. 10 - Voltage and current in the pump (Start-up transient).**

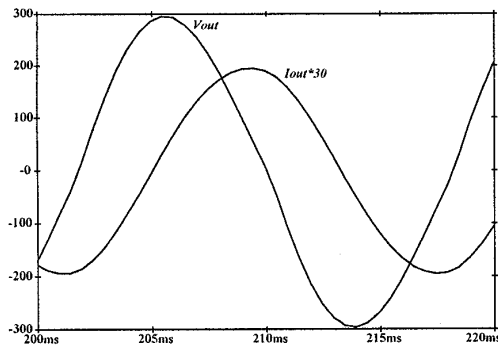


**Fig. 11 Voltage and current in the pump (Steady-state condition).**

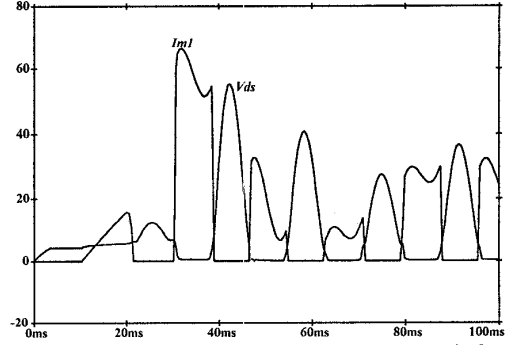


**Fig. 12 - Voltage and current in the main switches (Start-up transient).**

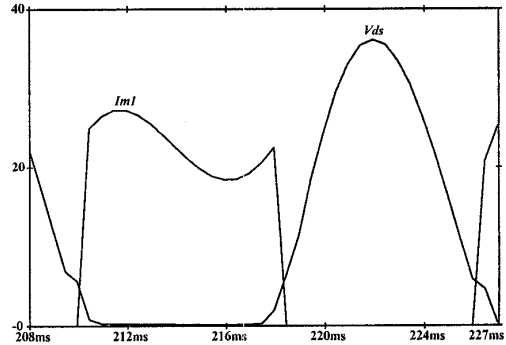


**Fig. 13 - Voltage and current in the main switches (Steady-state condition).**

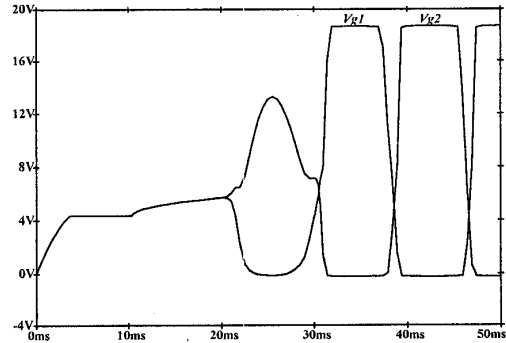


**Fig. 14 – Gate voltage in the switches (Start-up transient).**

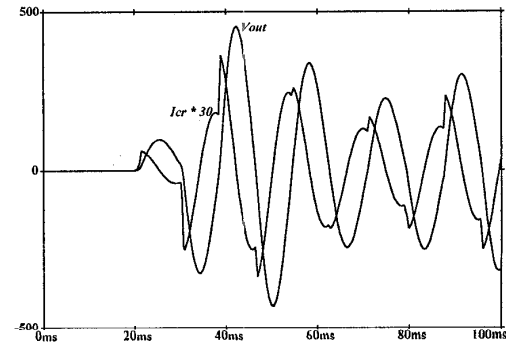


**Fig. 15 - Voltage and current in the resonant capacitor (Start-up transient).**

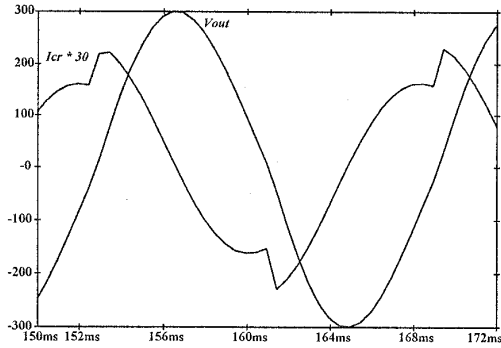


Fig. 16 - Voltage and current in the resonant capacitor (Steady-state condition).

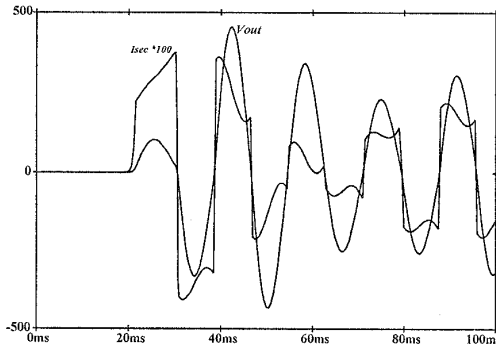


Fig. 17 - Voltage and current in the secondary side of the transformer (Start-up transient).

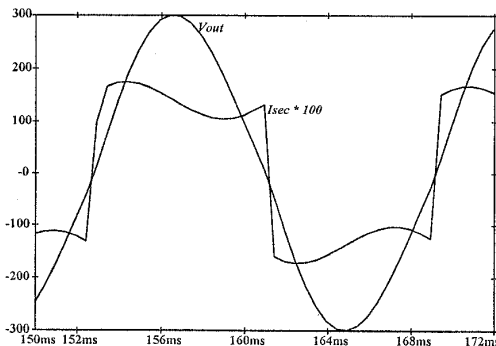


Fig. 18 - Voltage and current in the secondary side of the transformer (Steady-state condition).

From the results presented in this section we can observe that the voltage across the pump is practically sinusoidal with low harmonic distortion. The critical condition is the start-up transient of the converter, where the switches are submitted to a high voltage and current during approximately two cycles. The same overvoltage is observed at the output side. This information is very important for the design of the resonant capacitor.

## VI. EXPERIMENTAL RESULTS

A laboratory prototype rated 300W was built to evaluate the proposed circuit. The specifications are

given in section IV. Mosfet's were used for the main switches.

The main waveforms of the complete system are presented below:

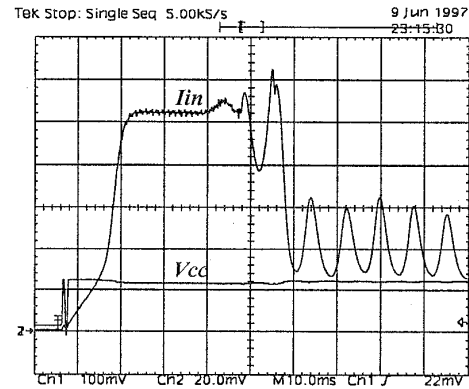


Fig. 19 - Voltage and current in the batteries (Start-up transient)  
Scales: 10V/div; 20A/div; 10ms/div.

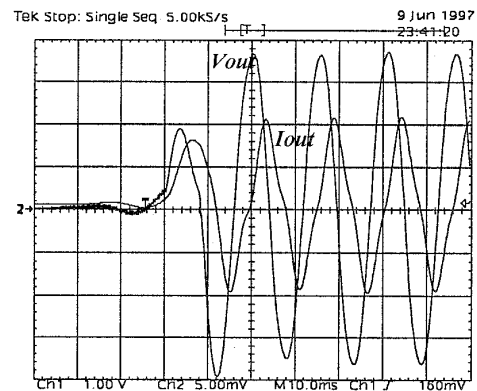


Fig. 20 - Voltage and current in the pump (Start-up transient)  
Scale: 100V/div; 5A/div; 10ms/div.

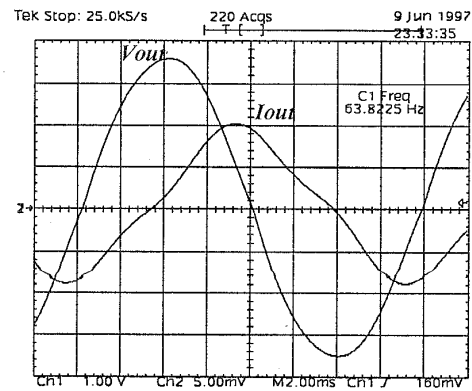
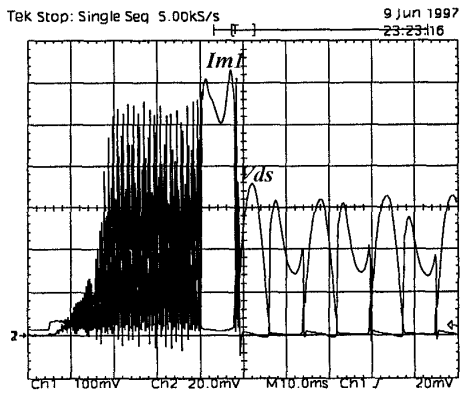
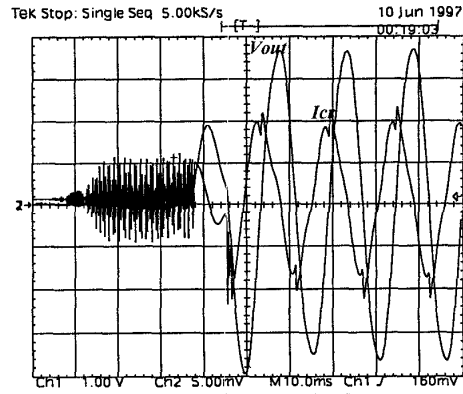


Fig. 21 - Voltage and current in the pump (Steady-state condition)  
Scale: 100V/div; 5A/div; 2ms/div.



**Fig. 22 - Voltage and current in the main switches (Start-up transient)**  
 Scale: 10V/div; 20A/div; 10ms/div.



**Fig. 25 - Voltage and current in the resonant capacitor (Start-up transient)**  
 Scale: 100V/div; 5A/div; 10ms/div.

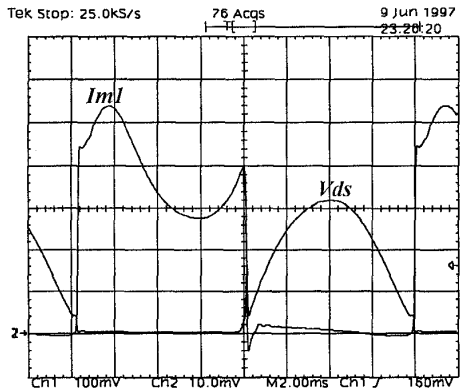


**Fig. 23 - Voltage and current in the main switches (Steady-state condition)**  
 Scale: 10V/div; 10A/div; 2ms/div.

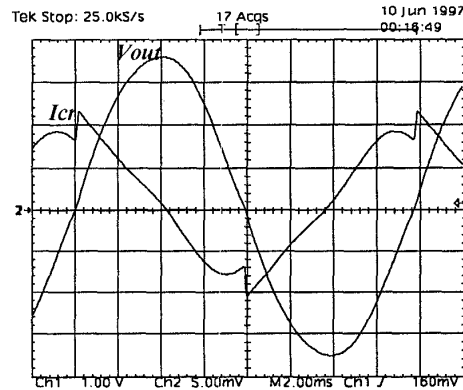


**Fig. 26 - Voltage and current in the resonant capacitor (Steady-state condition)**  
 Scale: 100V/div; 5A/div; 2ms/div.

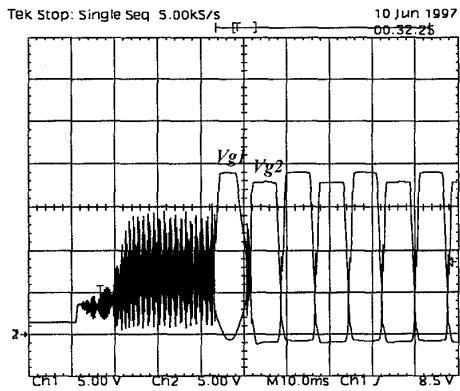


**Fig. 24 - Gate voltage in the switches (Start-up transient)**  
 Scale: 5V/div; 10ms/div.

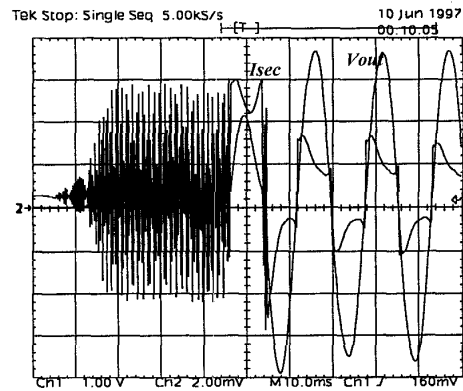


**Fig. 27 - Voltage and current in the secondary side of the transformer (Start-up transient)**  
 Scale: 100V/div; 2A/div; 10ms/div.

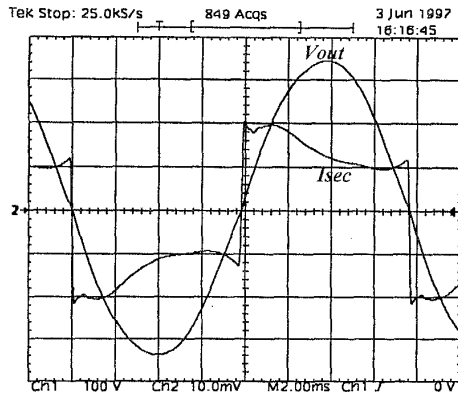


Fig. 28 - Voltage and current in the secondary side of the transformer (Steady-state condition)  
Scale: 100V/div; 1A/div; 2ms/div.

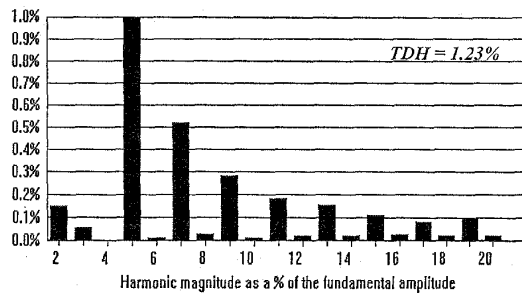


Fig. 29 - Output voltage harmonic analysis.

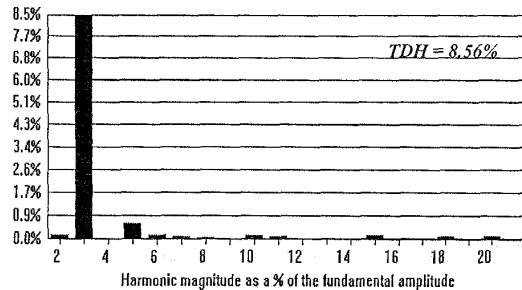


Fig. 30 - Harmonic analysis of the pump current.

The experimental results of the converter show that the voltage across the pump is practically sinusoidal, and the self-oscillator drive circuit presented a good behavior for this application. Besides, the over-voltage across the pump and the Mosfet's does not put in risk the structure. The start-up current of the converter is inside the limit specified by the manufacturer of the switches.

An efficiency of 80% was obtained at full load condition.

## VII. CONCLUSION

This paper has presented the analysis of a water pumping system from photovoltaic cells using a current-fed self-oscillator parallel resonant push-pull

inverter operating a under-water vibratory pump, for residential applications in rural areas. The converter shows to be extremely well adapted with this kind of pump, providing a sinusoidal voltage with low harmonic distortion without necessity of any type of modulation. According to the results obtained we have a DC-AC converter with the following features: it is particularly simple and robust; it uses low cost technology; it can operate with only one power processing stage; it has a simple control circuit with its terminals earthed in the same grounding; lower harmonic distortion of the load current, natural isolation and low number of control switches. Therefore, the authors believe that this topology can be very useful for some residential applications.

## VIII. REFERENCES

- [1] E. Muljadi, "PV Water pumping with a Peak-Power Tracker Using a Simple Six-Step Square-Wave Inverter", IEEE Trans. on Industry Applications, vol. 33, No. 3, May/June/1997, pp. 714-721.
- [2] M. Ohsato et al, "Battery Charging Characteristics From Photovoltaic Modules Using Resonant DC-DC Converter", IEEE - IPEC'90, Tokyo, April/1990, pp. 377-381
- [3] U. Herrmann, H. G. Langer & H. Vander Broeck, "Low Cost DC to AC Converter for Photovoltaic Power Conversion in Residential Applications", IEEE PESC'93, June/1993, pp. 588-594.
- [4] C. H. Lee, G. B. Joung, & G. H. Cho, "A Unity Power Factor High Frequency Parallel Resonant Electronic Ballast", IEEE 1990
- [5] G. W. Bruning, "A New High-Voltage Oscillator", IEEE Trans. on Industrial Electronics, vol. IE-33, No. 2, May/1986, pp. 171-175.
- [6] Pspice Circuit Analysis, Micosim Corporation, version 4.05, 1989